

MODELLING OF SINGLE-WALL CARBON NANOTUBES MECHANICAL BEHAVIOUR

N.A. SAKHAROVA^{*}, J.M. ANTUNES^{*†}, M.C. OLIVEIRA^{*}, B.M. CHAPARRO^{*†},
C.M.A. BRETT^{*} AND J.V. FERNANDES^{*}

^{*}CEMUC – University of Coimbra
Rua Luís Reis Santos, Pinhal de Marrocos, 3030-788 Coimbra, Portugal
e-mail: {nataliya.sakharova, marta.oliveira, valdemar.fernandes}@dem.uc.pt, cbrett@ci.uc.pt
<https://cemuc.dem.uc.pt/cemuc/>

[†]Escola Superior de Tecnologia de Abrantes
Instituto Politécnico de Tomar
Rua 17 de Agosto de 1808, 2200 Abrantes, Portugal
email: jorge.antunes@ipt.pt, bruno.chaparro@sapo.pt, <http://www.esta.ipt.pt>

Key Words: *Carbon Nanotubes, Numerical Simulation, Elastic Properties.*

Summary. In the present study a three-dimensional finite element model was used in order to evaluate the tensile and bending rigidities and, subsequently, Young's moduli of non-chiral and chiral single-walled carbon nanotubes. A comprehensive study on the influence of the nanotube wall thickness on the Young's modulus results was also carried out using data reported in the literature.

1 INTRODUCTION

Carbon nanotubes (CNTs) have attracted great research interest, because of their extraordinary mechanical, optical, thermal properties [1]. Although extensive experimental studies have been carried out to evaluate the mechanical properties of CNTs, there is a big inconsistency concerning the experimental results reported in the literature, owing to the complexity in performing the characterization of nanomaterials at the atomic scale. As a result, research in this field has been mainly driven by modelling and simulation of the behaviour of CNTs.

The theoretical approaches for modelling the CNTs behaviour can be divided into three categories: the atomistic approach, the continuum approach and the nanoscale continuum approach. A comprehensive critical review concerning the modelling of mechanical behaviour of carbon nanotubes has been undertaken in [2]. The atomistic modelling comprises classical molecular dynamics (MD) (see, for example, [3]), *ab initio* [4], tight-binding molecular dynamics (TBMD), local density, and the Morse potential model method. Atomistic modelling approaches are reliable and provide good predictions of the CNTs mechanical properties, but they are inappropriate for the simulation of the large systems, they are time-consuming and involve complex mathematical formulation. In recent years, the atomistic

methods have been progressively replaced by continuum methods, which are indicated for effective simulation of large atomic systems. The basic supposition of the continuum mechanics-based approaches (CM) is the modelling of CNT as a continuum structure (see, for example [5]). The nanoscale continuum modelling (NCM) can be considered as an adequate compromise to overcome the disadvantages of MD simulations, i.e. enormous computational efforts, and sensitivity of CM modelling in the precise evaluation of the CNTs mechanical properties. Moreover, in the NCM modelling, the discrete nature of the CNT lattice structure is preserved through replacing the carbon-carbon (C-C) bond by a continuum element, such as a truss, rod, spring or beam (see, for example [6-9]). The beam elements have received the most consideration in the research community because they are more convenient to use than other elements employed to substitute the C-C bond in NCM, and the models involving equivalent beams have led to more accurate results [9].

It has been established by various researchers (see for example, [9, 10]) that the carbon nanotube configuration (diameter and chirality of CNT) influences the value of the Young's modulus. Although the reported outcomes of the analytical and numerical studies towards the evaluation of the elastic properties of CNTs are encouraging, there are some divergences between the Young's modulus values reported in the literature [2]. Analysing these different results, it is seen that the discrepancies can be attributed to the use of different models, potential functions, force field constants, nanotube wall thickness, and even different modes of the definition for Young's modulus. For this reason, the study of the CNTs mechanical properties remains an important topic and needs further investigation.

The present study aims to contribute towards the study of the mechanical behaviour of single-walled carbon nanotubes (SWCNTs) using the equivalent continuum beam approach [9], i.e. each C-C bond in the nanoscale continuum model is replaced by a 3D beam element. The 3D FE model was used in order to evaluate the tensile and bending rigidities, and subsequently, Young's moduli of various SWCNT structures, as non-chiral (zigzag, $\theta = 0^\circ$ and armchair, $\theta = 30^\circ$) and the most numerous family of chiral ($\theta = 19.1^\circ$) ones, for a wide range of diameters.

2 ATOMIC STRUCTURE OF SWCNTS

There are several ways to view a single-walled carbon nanotube (SWCNT). A simple way to describe SWCNT is as a rolled-up graphene sheet, forming a hollow cylinder with end caps [11]. The cylinder is composed by hexagonal carbon rings, the end caps having pentagonal rings. The hexagonal pattern is repeated periodically leading to binding of each carbon atom to three neighbouring atoms with covalent bonds, which are very strong and play a significant role in outstanding mechanical properties of CNTs. The atomic structure of SWCNTs depends on the tube chirality, which is defined by the chiral vector \vec{c}_h and the chiral angle θ . A schematic illustration of an unrolled hexagonal graphene sheet is shown in Figure 1. The chiral vector is defined by the line connecting two crystallographically equivalent sites on a two-dimensional graphene structure. Mathematically, the chiral vector \vec{c}_h is defined by a pair of the lattice translation indices (n, m) and the unit vectors \vec{a}_1 and \vec{a}_2 of the hexagonal lattice as follows :

$$\vec{c}_h = n\vec{a}_1 + m\vec{a}_2 \quad (1)$$

where n and m are integers.

The length of the unit vector \vec{a} is defined as $a = \sqrt{3}a_{C-C}$ with the equilibrium carbon-carbon (C-C) covalent bond length a_{C-C} normally taken to be 0.1421 nm. The nanotube circumference, L , and diameter, d are defined as [11]:

$$L = |\vec{C}_h| = a\sqrt{n^2 + nm + m^2} \quad (2)$$

$$d = L/\pi$$

The chiral angle, θ , is given by [11]:

$$\theta = \sin^{-1} \frac{\sqrt{3}m}{2\sqrt{n^2 + nm + m^2}} \quad (3)$$

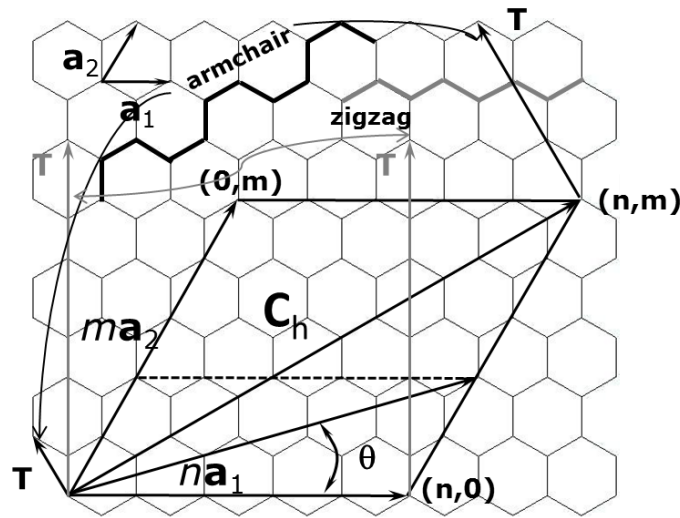


Figure 1: Schematic representation of the hexagonal lattice of the two-dimensional graphene sheet along with the definition of the chiral vector and description of SWCNTs formation

Generally, $n > m$ is used. Three main symmetry groups of SWCNTs exist. When $n = m$, the structure (n, n) is called armchair configuration; when $m = 0$, the structure $(n, 0)$ is called zigzag; when $n \neq m$, the structure (n, m) is chiral. These three major categories of SWCNTs are defined based on the chiral angle, θ , whose range lies between 0 and 30° , having exactly these values for CNTs referred to as armchair and zigzag, respectively. For θ different from 0 and 30° , the nanotubes are designated as chiral.

3 NUMERICAL SIMULATION AND ANALYSIS

3.1 FE modelling and configurations of SWCNTs

In the current work, the 3D FE model, which is able to assess the mechanical properties of SWCNTs, as proposed by Li and Chou [6] and developed by Tserpes and Papanikos [9], was adopted. The displacement of individual atoms of CNT under an external force is constrained by the C-C bonds. Therefore, the total deformation of the nanotube is the result of the

interactions between interatomic bonds. Since the C-C bonds are considered as connecting load-carrying elements, and the carbon atoms as joints of connecting elements, CNTs can be simulated as space-frame structures (see Figure 2). The modelling establishes the equivalence of the bond length, a_{c-c} , with the equivalent beam length, l , and the equivalence of the nanotube wall thickness, t_n , with the beam element thickness. Assuming the cross-sectional area of the beam element to be circular, the wall thickness, t_n , corresponds to the beam element diameter.

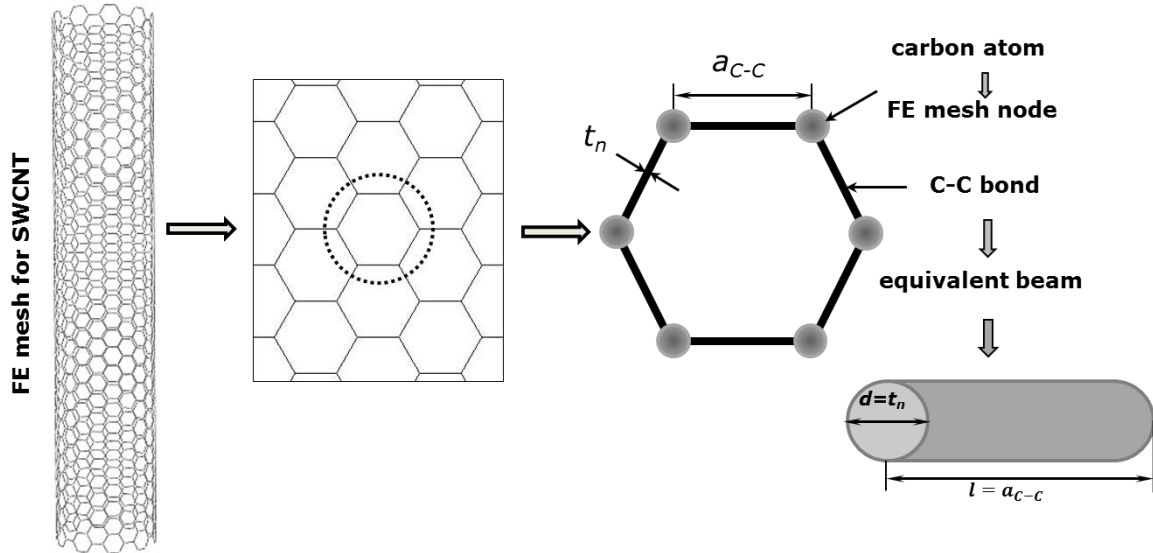


Figure 2: Modelling of SWCNT as a space-frame structure with beam elements substituting C-C bonds

The meshes for SWCNT structures used in finite element analyses were constructed using the academic software CoNTub 1.0 [12], which permits building the CNT structures for designing and investigation of new nanotube-based devices. This code is able to generate ASCII files, describing atom positions, which can be entered as input in available commercial or in-house FEA codes, in order to perform the simulation of mechanical tests. In order to convert ASCII files, from the CoNTub 1.0 program, into the format usable by the commercial FEA code ABAQUS®, the in-house application *InterfaceNanotubos* was developed.

3.2 Molecular interactions and equivalent properties of beam elements

As originally proposed [7], and subsequently developed [6], the elastic properties of the beam elements are determined by establishing the link between inter-atomic potential energies of the molecular structure and strain energies of the equivalent continuum structure comprising frame members (beams) undergoing axial and bending deformations. From the molecular point of view, CNTs can be envisaged as large molecules composed of carbon atoms. Thus, the atomic nuclei are considered as material points, and their movements are governed by a force-field produced by electron-nucleus and nucleus-nucleus interactions. The force-field is expressed in the form of the total potential energy, which is uniquely defined by the relative positions of the nuclei composing the molecule.

According to molecular dynamics, the total inter-atomic potential energy of a molecular

system is expressed as the sum of energy terms due to bonded and non-bonded interactions [13]:

$$U_{tot} = \sum U_r + \sum U_\theta + \sum U_\phi + \sum U_\omega + \sum U_{vdw} \quad (4)$$

where U_r , U_θ , U_ϕ , U_ω are energies associated with bond stretching, bending (bond angle variation), dihedral angle torsion, out-of plane torsion, respectively, and U_{vdw} is the energy associated with non-bonded van der Waals interaction. In the covalent system, which is the carbon nanotube, non-bonded interactions are negligible in comparison with bonded ones, and the main contribution to the total potential energy is from the first four terms of Eq. (4). The contributions of dihedral angle torsion and out-of plane torsion to total inter-atomic potential energy are insignificant, compared with contributions of other bonded interactions for a graphene subjected to small deflections, and the main contribution to inter-atomic potential energy is due to bond stretching and bending, as outlined in Figure 3. Consequently, under the assumption of small deformation, the energies associated with bond stretching and bending can be approximated by using harmonic functions [14]:

$$U_r = \frac{1}{2} k_r (\Delta r)^2 \quad (6)$$

$$U_\theta = \frac{1}{2} k_\theta (\Delta \theta)^2$$

where k_r , k_θ , are the bond stretching and bond bending force constants, respectively, and Δr and $\Delta \theta$ are the bond stretching increment and bond angle variation, respectively.

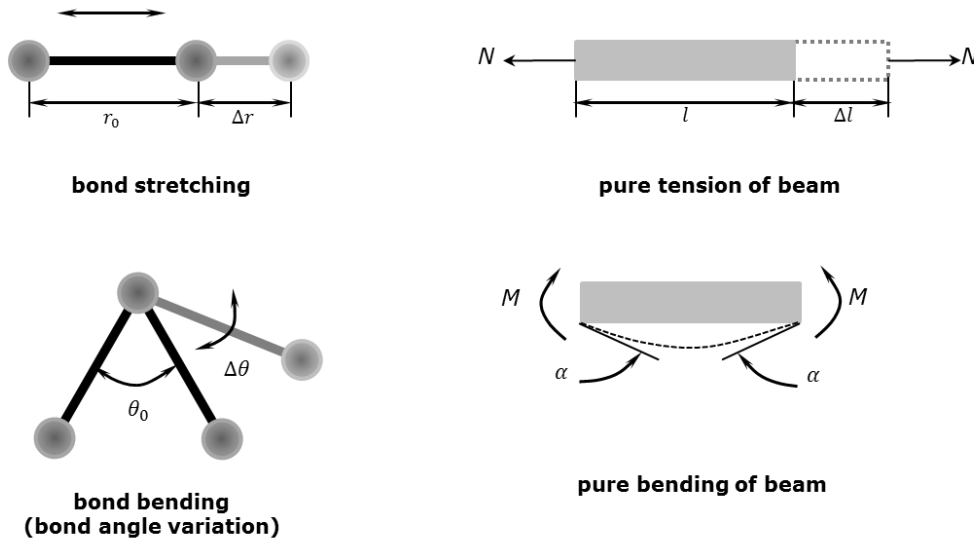


Figure 3: Equivalence between interatomic interactions in CNT and beam elements

Relationships between the sectional stiffness parameters in structural mechanics and force field constants in molecular dynamics are required for determination of the elastic properties of the beam elements. When a space-frame structure is subjected to deformation, strain

energies change. Thus, by establishing the equivalence of the energies associated with the interatomic interactions, through Eq. (6), and the energies associated with deformation of the structural elements (i.e. beams) of the space-frame structure, the elastic properties can be determined.

Classical mechanics gives the following expression for the strain energy, U_A , of a uniform beam with length, l , and cross-section area, A , under a pure axial force, N :

$$U_A = \frac{1}{2} \int_0^L \frac{N^2}{E_b A_b} dl = \frac{1}{2} \frac{N^2 l}{E_b A_b} = \frac{1}{2} \frac{E_b A_b}{l} (\Delta l)^2 \quad (7)$$

where Δl is the axial stretching deformation and E_b is the Young's modulus of the beam.

The strain energy, U_M , of a uniform beam under a pure bending moment, M , according to classical mechanics, is expressed as:

$$U_M = \frac{1}{2} \int_0^L \frac{M^2}{E_b I_b} dl = \frac{1}{2} \frac{E_b I_b}{l} (2\alpha)^2 \quad (8)$$

where α is the rotational angle at the ends of the beam and I_b is the moment of inertia of the beam.

The parameters U_r and U_A are stretching energies in molecular and structural systems, respectively, while U_θ and U_M represent the bending energies. Comparing Eqs. (6) with Eqs. (7) and (8), and assuming the equivalence of the rotational angle, 2α , to the total variation of the bond angle, $\Delta\theta$, as well the equivalence of Δl to Δr , direct relationships can be established between the structural mechanics parameters, $E_b A_b$, $E_b I_b$, and the force field constants, k_r , k_θ , [6]:

$$\begin{aligned} \frac{E_b A_b}{l} &= k_r \\ \frac{E_b I_b}{l} &= k_\theta \end{aligned} \quad (9)$$

Eq. (9) establishes the basis for the application of continuum mechanics to the analysis of the mechanical behaviour of CNTs, and provides the input for simulation of the CNTs as space-frame structures. The values of force constants and input data for the FE model are given in Table 1.

Table 1: Input parameters for FE model of SWCNTs.

Parameter	Value	Formulation
Force constant, k_r [15]	$6.52 \times 10^{-7} \text{ N nm}^{-1}$	–
Force constant, k_θ [15]	$8.76 \times 10^{-10} \text{ N}\cdot\text{nm}\cdot\text{rad}^{-2}$	–
C-C bond/beam length ($l = a_{C-C}$)	0.1421 nm	–
Diameter (d)	0.147 nm	$d = 4\sqrt{k_\theta/k_r}$
Cross section area, A_b	0.01688 nm^2	$A_b = \pi d^2/4$
Moment of inertia, I_b	$2.269 \times 10^{-5} \text{ nm}^4$	$I_b = \pi d^2/64$
Young's modulus, E_b	5488 GPa	$E_b = k_r^2 l / 4\pi k_\theta$
Tensile rigidity, $E_b A_b$	92.65 nN	$E_b A_b = k_r l$
Bending rigidity, $E_b I_b$	$0.1245 \text{ nN}\cdot\text{nm}^2$	$E_b I_b = k_\theta l$

3.3 Young's modulus of SWCNTs

The nanotube rigidities, $(EA)_{eq}$ and $(EI)_{eq}$, are required for the evaluation of the nanotube Young's modulus, E_{eq} . Considering a hollow cylindrical profile for the equivalent beam, which is appropriate because the CNT cross-sectional area is circular, the cross-sectional area of the equivalent hollow cylinder and secondary moment of inertia can be written as follows [16]:

$$\begin{aligned} A_{eq} &= \frac{\pi}{4} [(D_{eq} + t_{eq})^2 - (D_{eq} - t_{eq})^2] = \pi D_{eq} t_{eq} \\ I_{eq} &= \frac{\pi}{64} [(D_{eq} + t_{eq})^4 - (D_{eq} - t_{eq})^4] \end{aligned} \quad (10)$$

where D_{eq} and t_{eq} are the mean diameter and the thickness of the equivalent hollow cylinder, respectively. Assuming $t_{eq} = t_n$, the expression for D_{eq} can be derived from Eqs. (10):

$$\begin{aligned} (EI)_{eq}/(EA)_{eq} &= (D_{eq}^2 + t_n^2)/8 \\ D_{eq} &= \sqrt{(8(EA)_{eq}/(EI)_{eq}) - t_n^2} \end{aligned} \quad (11)$$

Thus, the Young's modulus of the equivalent beam can be calculated using the following expression taking into account the rigidities in tension and bending:

$$E_{eq} = (EA)_{eq}/A_{eq} = (EA)_{eq}/\pi t_n \sqrt{(8(EI)_{eq}/(EA)_{eq}) - t_n^2} \quad (12)$$

Whilst theoretical work has given values for the nanotube wall thickness that range from 0.066 to 0.69 nm (see, [3] and [7] respectively), in the current study the most widely used value $t_n = 0.34$ nm (which is equal to the interlayer spacing of graphite; see for example [19]) is adopted for the SWCNT wall thickness in order to enable comparison of the results with those available in literature.

4 RESULTS AND DISCUSSION

Different SWCNTs structures, such as chiral and non-chiral ones were assembled considering a wide range of chiral indices and diameters in order to cover a broad range of SWCNTs. The geometrical characteristics of SWCNTs used for the present FE analyses are summarised in the Table 2.

4.1 Rigidities of SWCNTs

As known from previous studies (see for example [16]), the mechanical behaviour of CNTs is length-independent, with the exception of very small lengths, so that modelling of the true length of the nanotube is not necessary. Thus, the evolution of the equivalent rigidities of SWCNTs was studied for the beam length at which the rigidities become stable, $L = 20$ nm. Figure 4a shows the evolutions of the equivalent tensile, $(EA)_{eq}$, and bending, $(EI)_{eq}$, rigidities as a function of the chiral indices, n , non-chiral SWCNTs, and the sum of chiral indices, $(n+m)$, for chiral SWCNTs. It is seen that the values of the tensile, $(EA)_{eq}$, and bending, $(EI)_{eq}$, rigidities of zigzag nanotubes are lower than the corresponding values for armchair nanotubes, and $(EA)_{eq}$ and $(EI)_{eq}$ of chiral nanotubes are lower than the values for

zigzag nanotubes. In order to clarify these trends, the values of the rigidities as a function of the SWCNT diameter, D_n , are plotted in Figure 4b. The FE results concerning the evolution of tensile and bending rigidities with nanotube diameter can be fitted by a quasi-linear trend for the case of tensile rigidity, $(EA)_{eq}$, and close to a cubic power for the case of bending rigidity, $(EI)_{eq}$, described by simple expressions as follows:

$$\begin{aligned} (EA)_{eq} &= \alpha(D_n - D_0) \\ (EI)_{eq} &= \beta(D_n - D_0)^3 \end{aligned} \quad (13)$$

These equations are of the same type as the ones previously proposed [16], but using the SWCNT diameter, D_n , instead of the chiral index, n .

Table 2: Geometrical characteristics of SWCNTs studied

SWCNT type	(n, m)	D_n , nm	θ°	
non-chiral	armchair	(3, 3)	0.407	30
		(5, 5)	0.678	
		(10, 10)	1.356	
		(15, 15)	2.034	
		(20, 20)	2.713	
	zigzag	(5, 0)	0.392	0
		(10, 0)	0.783	
		(15, 0)	1.175	
		(20, 0)	1.566	
		chiral family $\theta=19.1$	(4, 2)	
(6, 3)	0.622			
(8, 4)	0.829			
(10, 5)	1.036			
(12, 6)	1.243			
(14, 7)	1.450			
(16, 8)	1.657			
(18, 9)	1.865			
(20, 10)	2.072			
(22, 11)	2.279			
(24, 12)	2.486			

The fitting parameters α , β and D_0 are given in Table 3, for the current work, along with those calculated based on the results of previous work ([16] and [17]). Eqs. (13) permit accurate determination of the rigidity values for the chiral and non-chiral SWCNTs. For SWCNTs with diameter $D_n > 0.4$ nm, the mean difference between the values of $(EA)_{eq}$, obtained from Eq. (13) and the values obtained from FE analysis, is 0.05% for armchair, 0.03% for zigzag and 0.07% for chiral SWCNTs. The differences between the values of $(EI)_{eq}$ estimated by Eq. (13) and those obtained from FE analysis are slightly higher due to the cubic power of D_n , viz. 3.02% for armchair, 2.21% for zigzag and 1.70% for chiral SWCNTs. The larger deviation from FE results is observed for SWCNTs with smaller diameters. The maximum differences in the bending rigidity of SWCNTs with $D_n < 0.4$ nm

are 7.52%, 5.85% and 5.34 for armchair, zigzag and chiral nanotubes, respectively.

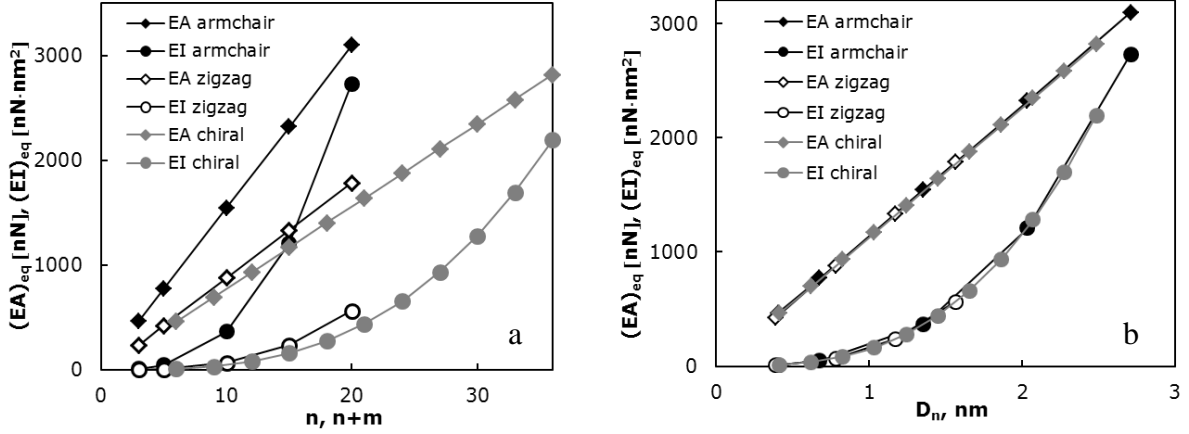


Figure 4: Evolution of the tensile, $(EA)_{eq}$, and bending, $(EI)_{eq}$, rigidities as a function of the chiral index, n , or $(n+m)$ (a) and nanotube diameter, D_n for armchair, zigzag and chiral $\theta = 19.1^\circ$ SWCNTs

Table 3: Fitting parameters

Parameter	Current study			Papanikos <i>et al.</i> [16]		Chang and Gao [17]	
	armchair	zigzag	chiral	armchair	zigzag	armchair	zigzag
α (nN/nm)	1140.6	1133.7	1131.4	1119.2	1137.1	1135.5	1147.1
β (nN/nm)	137.91	146.59	143.27	139.05	146.00	–	–
D_0 (nm)	$5.2 \cdot 10^{-8}$	$6.0 \cdot 10^{-8}$	$1.7 \cdot 10^{-7}$	0	0.03	–	–

4.2 Young's modulus of SWCNTs

Using relations (13) for the tensile and bending rigidities, Eq. (12) can be transformed into the equation:

$$E_{eq} = (EA)_{eq}/A_{eq} = \alpha(D_n - D_0)/\pi t_n \sqrt{8\beta/(\alpha(D_n - D_0)^2) - t_n^2}, \quad (14)$$

which allows easy assessment of the Young's modulus of the equivalent beam, knowing the SWCNT diameter, wall thickness and fitting parameters from Table 3.

The wall thickness plays an important role in predicting the elastic modulus of SWCNTs (see, for example [9]). The influence of the value of SWCNT wall thickness on the value of the Young's modulus was performed in order to assess the accuracy of the FE model used in the present work in comparison with the results of the parametric studies reported in the literature. Figure 5a presents the effect of the nanotube wall thickness (for the t_n values available in the literature) on their Young's modulus, evaluated by Eq. (14), for the case of armchair SWCNTs.

It can be seen that the Young's modulus is strongly dependent on the tube wall thickness: the greater the wall thickness, t_n , the smaller the Young's modulus, as previously observed [7, 9, 18]. For comparison purposes, Figure 5b shows the variation of the Young's modulus of the (10, 10) SWCNT ($D_n = 1.356$ nm), evaluated by the current FE model, with the inverse wall thickness, plotted along with the Young's modulus values available in the literature and

obtained by different methods, i.e. using the MD approach [3, 4, 18], CM method [5], and NCM models [7, 9, 19] where the C-C bonds were simulated using truss, non-linear connectors and beam elements, respectively.

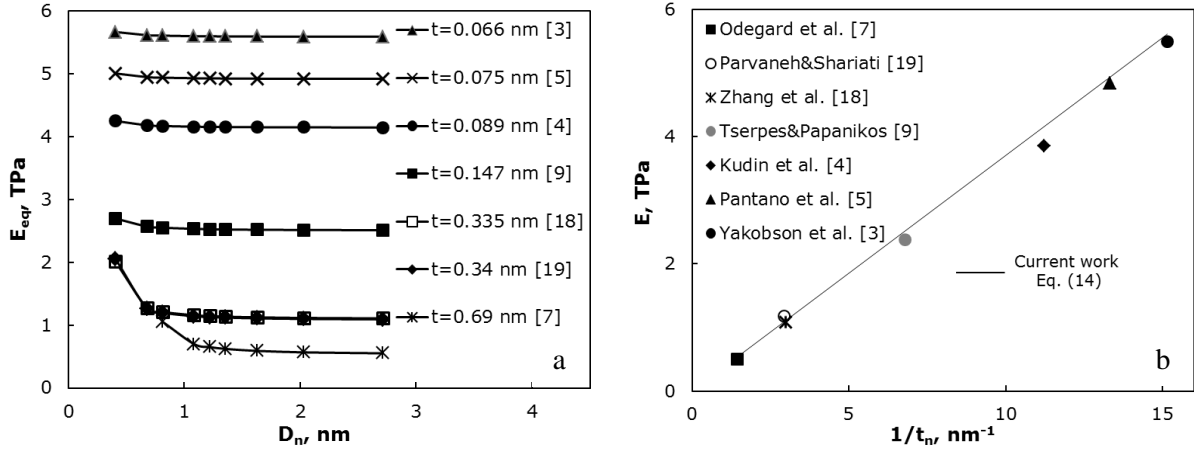


Figure 5: Comparative study: (a) evolution of SWCNTs Young's modulus with nanotube diameter for different wall thicknesses, (b) evolution of the Young's modulus of (10, 10) SWCNT with inverse wall thickness (values of D_n and fitting parameters from Tables 2 and 3, respectively)

Good agreement between the current Young's modulus results and the Young's modulus obtained by all of the other methods is observed. Figure 5b shows that the Young's modulus value, as described by Eq. (14), is closely proportional to the inverse of the wall thickness as was previously stated [9].

As reported in the literature [9, 10, 16], the SWCNT Young's modulus depends on the diameter and chirality. In Figure 6, the Young's modulus results in the form of the product Et_n , the assessment of which facilitates comparison of the results, are shown as a function of the nanotube diameter. For all SWCNT configurations studied, the Young's modulus values decrease with increasing nanotube diameter for small CNT diameters, $D_n \leq 0.828$ nm, then, with increase of nanotube diameter, the rate of decrease of the Young's modulus slows down and for $D_n \geq 1.221$ nm, the Young's modulus converges to an almost constant value of about 1.08 TPa.

Reviewing the data available in the literature, concerning the prediction of the CNTs elastic moduli, it can be seen that there are some discrepancies not only in the Young's modulus values, but also in the trend of the Young's modulus variation with the nanotube diameter. Three different trends are reported: (i) the Young's modulus decreases with increasing nanotube diameter (Figure 6a); (ii) the Young's modulus is independent of the nanotube diameter and (iii) the Young's modulus increases with increase of the nanotube diameter (Figure 6b). Inconsistencies in trends appear for small SWCNT diameters, and for big diameters, the Young's modulus approaches the value established for graphene sheets, whatever the evaluation method used. The differences in the trends observed can be attributed to dissimilar analytical and modelling approaches used by different authors.

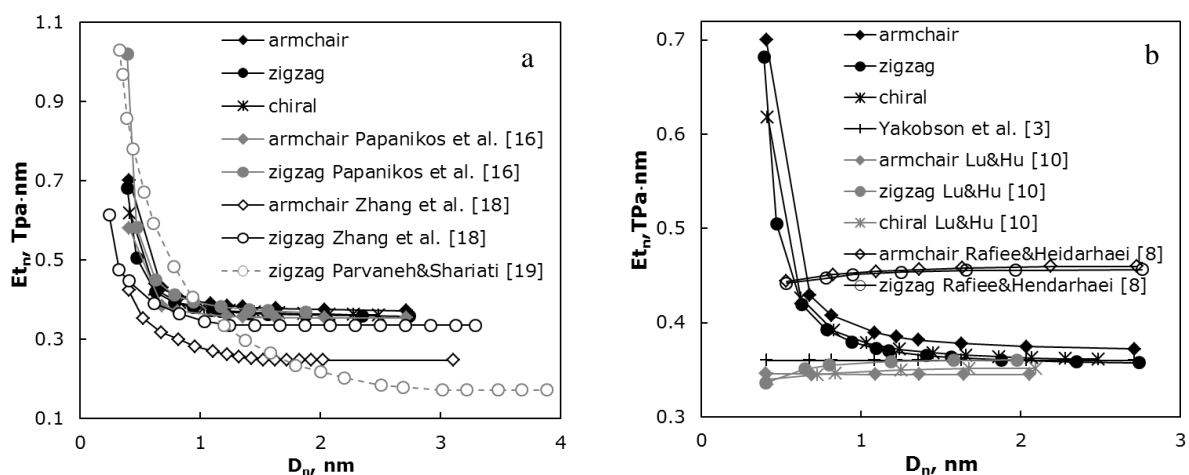


Figure 6: Comparative study of the evolution of the averaged SWCNTs' Young's modulus with the nanotube diameter: (a) "decreasing" trend; (b) "steady" and "increasing" trends

Concerning the effect of the nanotube chirality on the Young's modulus, the current results show identical tendencies in its evolution for armchair, zigzag and chiral SWCNTs, the Young's modulus of armchair SWCNT being slightly higher than that of chiral SWCNT.

5 CONCLUSIONS

- The tensile and bending rigidities of non-chiral and chiral SWCNTs are sensitive to the nanotube chirality and equations allowing direct relation of both rigidities with the nanotube diameter have been obtained. The accuracy of these relationships was verified using results available in the literature.
- These relationships, obtained for the tensile and bending rigidities, permit rapid evaluation of the SWCNT Young's modulus.
- The Young's modulus values for different nanotube wall thicknesses are inversely proportional to the wall thickness, the trend and quantitative values being in good agreement with the results published by other authors. Thus, this study also provides data for benchmark models.
- A "decreasing" trend of the Young's modulus variation with increasing SWCNT diameter was found. It can be concluded that the uncertainty associated with the Young's modulus results for SWCNTs with small diameters requires development of appropriate methodology for such cases.

ACKNOWLEDGEMENTS

This research work is sponsored by national funds from the Portuguese Foundation for Science and Technology (FCT) via the projects PTDC/EME-TME/122472/2010 and PEst-C/EME/UI0285/2013 and by FEDER funds via "Programa Operacional Factores de Competitividade" – COMPETE, under the project CENTRO-07-0224_FEDER-002001 (MT4MOBI). All financial support is gratefully acknowledged.

REFERENCES

- [1] Robertson J., Realistic applications of CNTs. *Mater. Today* (2004) **7**: 46–52.
- [2] Rafiee R. and Moghadam R.M. On the modeling of carbon nanotubes: A critical review. *Compos. Part B-Eng.* (2014) **56**: 435–449.
- [3] Yakobson B.I., Brabec C.J., Bernholc J. Nanomechanics of carbon tubes: instabilities beyond linear response. *Phys. Rev. Lett.* (1996) **76**: 2511–2514.
- [4] Kudin K.N., Scuseria G.E., Yakobson B.I. C₂F, BN and C nanoshell elasticity from *ab initio* computations. *Phys. Rev. B* (2001) **64**:235406.
- [5] Pantano A., Parks D.M., Boyce M.C. Mechanics of deformation of single-and multi-wall carbon nanotubes. *J. Mech. Phys. Solids* (2004) **52**:789–821.
- [6] Li C. and Chou T.W. A structural mechanics approach for the analysis of carbon nanotubes. *Int. J. Solids Struct.* (2003) **40**:2487-2499.
- [7] Odegard G.M., Gates T.S., Nicholson L.M., Wise K.E. Equivalent continuum modeling of nano-structured materials. *Compos. Sci. Technol.* (2002) **62**: 1869–1880.
- [8] Rafiee R. and Heidarhaei M. Investigation of chirality and diameter effects on the Young's modulus of carbon nanotubes using non-linear potentials. *Compos. Struct.* (2012) **94**: 2460–2464.
- [9] Tserpes K.I. and Papanikos P. Finite Element modeling of single-walled carbon nanotubes. *Compos. Part B-Eng.* (2005) **36**: 468-477.
- [10] Lu X. and Hu Z. Mechanical property evaluation of single-walled carbon nanotubes by finite element modeling. *Compos. Part B-Eng.* (2012) **43**: 1902-1913.
- [11] Dresselhaus M.S., Dresselhaus G., Saito R. Physics of carbon nanotubes. *Carbon* (1995) **33**: 883-891.
- [12] Melchor S. and Dobado J.A. CoNTub: an algorithm for connecting two arbitrary carbon nanotubes. *J. Chem. Inf. Comp. Sci.* (2004) **44**: 1639-1646.
- [13] Rappe A.K., Casemit C.J., Colwell K.S., Goddard W.A., Skiff W.M. UFF, a full periodic-table force-field for molecular mechanics and molecular dynamics simulations. *J. Am. Chem. Soc.* (1992) **114**: 10024-10035.
- [14] Gelin B.R. Molecular modeling of polymer structures and properties. Cincinnati (OH): Hanser/Gardner Publishers (1994).
- [15] Cornell W.D., Cieplak P., Bayly C.I., Gould I.R., Merz K.M., Ferguson D.M., et al. A second generation force-field for the simulation of proteins, nucleic acids and organic molecules. *J. Am. Chem. Soc.* (1995) **117**: 5179-197.
- [16] Papanikos P., Nikolopoulos D.D., Tserpes K.I. Equivalent beams for carbon nanotubes. *Comput. Mater. Sci.* (2008) **43**: 345-352.
- [17] Chang T. and Gao H., Size-dependent elastic properties of a single-walled carbon nanotube via a molecular mechanics model. *J. Mech. Phys. Solids* (2003) **51**: 1059-1074.
- [18] Zhang H.W., Wang J.B., Guo X. Predicting the elastic properties of single-walled carbon nanotubes. *J. Mech. Phys. Solids* (2005) **53**: 1929–1950.
- [19] Parvaneh V. and Shariati M. Effect of defects and loading on prediction of Young's modulus of SWCNTs. *Acta Mech.* (2011) **216**: 281–289.